Forward-Look Wind-Shear Detection for Microburst Recovery

David A. Hinton*
NASA Langley Research Center, Hampton, Virginia 23665

An effort is in progress by NASA, the Federal Aviation Administration, and the industry to reduce the threat of convective microburst wind-shear phenomena to aircraft. This paper describes an effort to quantify the benefits of forward-look sensing and to develop and test a candidate set of strategies for recovery from inadvertent microburst encounters during the landing approach. Initial development of recovery strategies was performed in batch simulation prior to piloted simulation evaluation using a full dynamic airplane model. The results of this effort indicate that the factor that most strongly effects a microburst recovery is the time at which the recovery is initiated. Improving the alert time by 5 s generally provided a greater recovery performance increase than could be achieved by changing the recovery strategy. Forward-look alerts given 10 s prior to microburst entry permitted recoveries to be made with negligible altitude loss.

Nomenclature

F = wind-shear hazard index
g = gravitational acceleration
Href = reference altitude for recovery strategies
V = airplane airspeed
W_h = vertical wind component, updraft positive
W_x = horizontal wind component, along the airplane ground track

Introduction

NUMEROUS air carrier accidents and incidents have resulted from inadvertent encounters with the atmospheric wind shear associated with microburst phenomena, in some cases resulting in heavy loss of life. A microburst is a strong, localized downdraft that strikes the ground, producing winds that diverge radially from the impact point. An airplane penetrating the center of a symmetric microburst will initially encounter an increasing head wind, followed by a strong downdraft and rapidly increasing tail wind. The effects of the downdraft and increasing tail wind may easily exceed the performance capabilities of the airplane, causing unavoidable ground contact.

NASA and the Federal Aviation Administration (FAA) are addressing this hazard through the Integrated Wind-Shear Program. The goal is to reduce the hazard of low-level wind shear to aircraft operations through improved airborne and ground-based wind-shear detection systems, crew alerting and flight guidance systems, and training and operating procedures. NASA is investigating the airborne aspects of the problem through hazard characterization, sensor technology, ground information fusion, and flight management systems.

Previous research has shown the performance available from an airplane following an optimal trajectory[1] when full knowledge of the microburst flowfield is known. The application of these optimal recovery concepts to practical recovery guidance laws was studied,[2] and the performance of those guidance laws in piloted operations, in the takeoff encounter case, was evaluated in the simulator study described in Ref. 3. The studies described in Refs. 2 and 3 showed that advanced guidance laws enabled recovery to take place at higher minimum altitudes than with baseline constant pitch techniques, but that recovery altitude was very sensitive to small deviations in airplane pitch history. In piloted simulation tests, the performance differences between various recovery strategies were statistically insignificant. This result emphasized the need for microburst avoidance.

Two levels of microburst avoidance are possible: 1) totally avoid an encounter with the microburst phenomena, and 2) avoid placing an aircraft in a critical low-energy situation by initiating a recovery procedure prior to microburst entry. The first level of avoidance is preferred, but requires a higher degree of sensor development than the second level. Sensor development efforts have raised the issues of how much forward-look distance is necessary to ensure airplane survival and how recovery procedures will be effected by forward-look sensing. This paper describes an effort aimed at quantifying the benefits of relatively short range forward-look sensing and developing compatible recovery guidance concepts for the approach-to-landing case wind-shear encounter.

Batch Simulation

Initial quantification of forward-look benefits and development of recovery strategies were performed in batch simulation prior to piloted simulation evaluation using a full dynamic airplane model. The batch simulation consisted of a point-mass airplane model, an analytical microburst model, and a simple wind-shear detection scheme.

Airplane Model

The airplane model was based on a Boeing 737-100 flying in a vertical plane. The gross weight was set at 90,000 lb and sea level standard atmospheric conditions were assumed. The change of lift and drag coefficients with landing gear and flap actuation were modeled. For landing approach, autothrottle and glide slope tracking algorithms were implemented. The maximum available (rated) thrust of the model was 24,000 lb. The rate of change of thrust was limited to 6000 lb/s.

Microburst Model

The microburst model[4] represents an axisymmetric stagnation point flow that satisfies mass continuity and includes boundary-layer effects near the ground. The boundary-layer effects and spatial variation in outflow and downflow closely match real-world observations. The microburst has a maximum outflow of 37 kt at an altitude of 120 ft and at a radius of 2391 ft. The diameter of this microburst is on the short

Presented as Paper 89-3325 at the AIAA Flight Simulation Technologies Conference, Boston, MA, Aug. 14-16, 1989; received Nov. 13, 1989; revision received Dec. 8, 1990; accepted for publication Dec. 12, 1990.

*Aerospace Engineer.

length side of those that have been measured and encountered by aircraft, which tends to increase the aviation hazard, and the severity of the modeled shear is representative of microbursts that have caused aircraft accidents. As a consequence of the boundary-layer effects and altitude dependency of the downflow, the apparent severity of the shear is dependent on the location of the microburst relative to the landing runway and, hence, the altitude of the encounter.

Wind-Shear Detection

Wind-shear detection logic was used to activate the recovery control laws. The detection was based on the *F*-factor of the wind shear.[2] *F*-factor is defined as

$$F = \frac{\dot{W}_x}{g} - \frac{W_h}{V}$$

The *F*-factor scales directly with the still-air climb gradient capability of an airplane to give the climb gradient that can be maintained at a constant airspeed in the presence of a wind shear (referred to as the potential flight-path angle). An airplane with a normal climb angle of 0.15 rad subjected to an *F* of 0.15 would not be able to climb while maintaining speed and would have a potential flight-path angle of zero. The *F*-factor, appropriately filtered for turbulence rejection, is used in currently certified airborne wind-shear detection systems.

An *F* threshold of 0.15 was used to determine when the shear had been entered. This value is the maximum threshold permitted in certified wind-shear detection systems. The threshold *F* does not occur at a particular spatial location in the microburst model, but depends on airplane altitude, flight path, and airspeed. Variable time advance and delay was implemented to simulate forward-look sensors and reactive device delays. The advance is defined as the number of seconds that the alert is given before the threshold *F* would have been exceeded if no alert had been given. The delay is defined as the number of seconds that the alert is given after the threshold *F* is exceeded. A delay of 5 s is considered to approximate the response of realizable reactive detection systems.

Candidate Wind-Shear Recovery Strategies

Prior to wind-shear encounter, the aircraft tracked a 3-deg glide slope and the autothrottle attempted to maintain a reference speed of 137 kt. Wing flaps were positioned to 25 deg and the landing gear was down. The recovery strategy under test was activated upon detection of the wind shear.

Of the various recovery strategies tested, three are discussed in the following. The control law for each strategy limited the target pitch attitude to the value that would place the airplane at the stick shaker angle of attack and the pitch rate was limited to 3 deg/s. During escape maneuvers, each recovery strategy left the wing flap and landing gear positions unchanged and maximum rated thrust was applied. This is in accordance with the recovery procedures currently being taught to airline crews.

Manual Strategy

This strategy is currently in use by the airline industry.[5] Since this strategy was designed to be manually flown in the absence of guidance commands, the exact procedure used will vary slightly from pilot to pilot. For this effort, the manual recovery was approximated by initially rotating the airplane to a pitch attitude of 15 deg. This pitch attitude was maintained if it produced a zero or positive flight-path angle. If 15 deg of pitch was insufficient to maintain level flight, however, the control law would further increase pitch in an attempt to maintain level flight.

Flight-Path Angle Strategy

This strategy required the airplane to fly a flight-path angle that was a function of altitude, wind shear, *F*-factor, and available airplane performance. When the potential flight-path angle was positive, that climb gradient was maintained. When the potential flight-path angle was negative, the target climb gradient was altitude dependent. Below a reference altitude *H*ref, the strategy attempted to climb regardless of wind-shear strength, under the assumption that obstacles must be cleared. The target flight-path angle was 0.03 rad at ground level, reducing linearly to level fight at *H*ref. Above *H*ref, the strategy maintained one-half the potential flight-path angle. This permitted a descent to be maintained at the higher altitudes in order to reduce the rate at which airspeed was lost. *H*ref was set to 100 ft for reactive alert recoveries and 400 ft for forward-look alert recoveries. These altitudes provided the best overall performance in preliminary data runs. Both the positive and negative flight-path angle target values were limited to 0.06 rad to prevent excessive climb or descent rates during the recovery. The flight-path angle was further limited to prevent descent below the glide slope.

Glide Slope Strategy

This strategy attempted to emulate the characteristics of the optimal approach abort trajectories described in Ref. 6. That effort showed that the optimal recovery trajectory initially produced a descent and later transitioned to level flight. The level flight path was flown until exiting the wind shear. For this study, that trajectory was approximated by initially tracking the glide slope, at maximum rated thrust, until the altitude reached a reference altitude *H*ref. The value of *H*ref was 100 ft for reactive alert recoveries and 500 ft for forward-look alert cases. After reaching *H*ref, the strategy attempted to maintain a zero flight-path angle until exiting the shear. The glide slope was chosen as the descent angle to provide obstacle clearance during the recovery.

Real-Time Simulation

Piloted Simulator

The NASA Langley six-degree-of-freedom visual motion simulator was utilized in the piloted tests. The simulator provided a generic transport airplane flight deck equipped with conventional electromechanical instrumentation, an out-the-window display of terrain, and audio cues for wind and engine noise. The recovery guidance was presented on the attitude-director indicator (ADI) by conventional dual cue command bars. A pitch target was continuously calculated to accomplish the recovery and the pitch command bar was driven to that value. The roll command bar was driven by bank angle, so that the command was nulled when the wings were level and full-scale deflection occurred at a bank angle of 60 deg. A fast/slow indicator in the ADI display was driven by speed error, with full-scale deflection occurring at 10 kt of error.

Pilot control input was through a wheel and control column hydraulically loaded in pitch and roll, hydraulically loaded rudder pedals, and independent throttle levers. A stick shaker function was implemented on the control column. The simulator was driven with a full nonlinear math model of a Boeing 737-100 airplane. The model included lift and drag coefficient data to 24-deg angle of attack and the effects on those coefficients of pitch rate, control deflection, and ground effect. The aircraft was flown in the landing configuration at a gross weight of 90,000 lb.

Microburst Models

Two microburst models were utilized in the piloted simulation. The first was the same analytical model used for the batch simulation effort. The second model was a numeric representation of a microburst as generated by the Terminal Area Simulation System (TASS) program.[7,8] The TASS program implements a numeric atmospheric simulation, which determines parameters such as temperature, wind components, pressure, and liquid water content at grid points within a cube of airspace during the evolution of a microburst. For

this effort, the TASS model was initialized with the atmospheric conditions that produced a microburst at the Dallas-Fort Worth (DFW) airport in August, 1985. The resulting TASS output closely resembled the microburst involved in the DFW accident.

The two microburst models differ primarily in the scale of the event and in the precursors entering the microburst. The TASS model is a large-scale event, with the performance-decreasing wind change taking place over a distance of about 12,000 ft, or more than double the corresponding distance in the analytical model. Prior to entering the performance-decreasing region, both models include a performance-increasing region. This region involves only an increasing head wind in the analytical model. In the TASS model, the performance-increasing region involves both an increasing head wind and a strong updraft.

Wind-Shear Detection

Both reactive and forward-look detection capabilities were used. The *F*-factor was used in the implementation of both detection types. In the reactive detection case, knowledge of the local horizontal and vertical wind was used to calculate the *F*-factor. The reactive alert was given when the calculated *F*-factor exceeded a threshold value for 5 s. In the forward-look detection case, the horizontal *F*-factor component was calculated using wind divergence information at a detection point ahead of the airplane and the vertical *F*-factor component was derived from a vertical wind estimator algorithm, which assumed microburst symmetry and mass continuity in the flow. The detection point was located along the instantaneous flight-path vector of the airplane, at a distance corresponding to 10 s of flight time. The detection threshold value of the *F*-factor was set at 0.12 for the reactive alert. This threshold is typical of presently certified reactive wind-shear detection systems. To compensate for known error sources in the forward-look *F*-factor estimator and to achieve a forward alert 10–15 s in advance of the reactive alert, the forward-look detection threshold was set at 0.10.

Alerts were presented both visually and aurally. A red annunciator light directly above the ADI and a warbling tone indicated a reactive alert. An amber light above the right corner of the ADI and a steady tone indicated a forward-look alert. Upon receiving a forward-look alert, the escape guidance was activated by the pilot pressing a throttle-mounted takeoff-go-around (TOGA) switch. Upon receiving a reactive alert, the flight director automatically switched to the escape guidance.

Experimental Conditions

Three microburst scenarios were used for the statistical analysis. In each case, the microburst was located on the extended runway centerline and the run began with the airplane on localizer and glide slope at an altitude of 1200 ft. One scenario positioned the core of the analytical microburst 1640 ft from the runway. A second scenario positioned the same microburst at an increased distance of 3600 ft from the runway. The encounter altitudes resulting from these two locations exposed the airplane to the region of maximum *F*-factor in the analytical microburst and provided a difficult piloting task due to the low encounter altitude. The third scenario positioned the TASS model 1640 ft from the runway. The matrix used for data analysis consisted of three repetitions of three microburst scenarios, three recovery strategies, and two alert times (reactive only and forward look) for a total of 54 runs. Another 11 runs, not included in the analysis, were inserted throughout the matrix to provide variability to the pilots by presenting different microburst geometries and locations.

A total of seven research and airline pilots participated in the study. The average amount of turbojet experience was over 5000 h. Five of the seven pilots had completed the FAA wind-shear training aid program. The piloting task was identical to the batch simulation runs, in that the same approach speed and configuration was used, recovery was not initiated until receiving a wind-shear alert, and aircraft configuration was not changed during the recovery.

Results

Batch Simulation Recovery Altitude Performance

In each batch run, the airplane was initialized 4000 ft from the center of the microburst. The geometry of the microburst encounter was varied by changing the initial altitude of the airplane. The initial altitude, wind-shear encounter altitude, recovery altitude, and alert time for a subset of the runs made are shown in Table 1. The encounter altitude is the altitude at which the wind shear was detected and the recovery initiated, and the recovery altitude is the lowest altitude during the encounter. The initial altitudes vary from 300 to 700 ft above ground level in 100-ft increments, and the alert time varies from a 10-s forward look to a 10-s delay in 5-s increments.

Of the factors explored, the factor that produced the greatest improvement in recovery altitude was the alert time. The improvement in recovery altitude with each 5-s improvement in the alert time was generally greater than the difference in

Table 1 Batch run recovery altitudes

Initial altitude, ft	Strategy	Alert time, s −10	−5	0	+5	+10
		(59)[a]	(111)	(159)	(203)	(250)
300	Manual	21	39	18	22	153
	Flight path	21	40	81	120	239
	Glide slope	21	53	84	134	239
		(161)	(212)	(261)	(306)	(354)
400	Manual	12	13	20	88	312
	Flight path	12	31	85	198	344
	Glide slope	12	31	75	187	344
		(264)	(315)	(363)	(411)	(460)
500	Manual	3	11	45	226	450
	Flight path	3	30	148	329	404
	Glide slope	3	30	146	286	450
		(366)	(416)	(466)	(515)	(566)
600	Manual	41	57	154	388	555
	Flight path	41	108	271	403	474
	Glide slope	41	108	240	468	487
		(466)	(516)	(568)	(619)	(672)
700	Manual	149	160	288	553	655
	Flight path	149	241	395	469	580
	Glide slope	149	241	339	483	483

[a]Numbers in parenthesis indicate the wind-shear encounter altitude for a particular initial altitude and alert time.

Table 2 Average recovery altitudes in piloted runs

Shear scenario	Recovery strategy: Manual Reactive alert[a]	Manual Forward[b] alert	Flight-path angle Reactive alert	Flight-path angle Forward alert	Glide slope Reactive alert	Glide slope Forward alert
TASS	206	503	134	472	210	481
Analytical at 1640 ft	62	309	39	307	62	303
Analytical at 3600 ft	53	409	53	401	81	397
All shears	107	407	75	393	118	394
All runs this strategy	257		234		256	

[a]All reactive alerts are 100 ft. [b]All forward-look alerts are 398 ft.

performance between recovery strategies. Depending on the initial altitude, the recovery altitude increase ranged from 114 to 498 ft when the alert time was improved from −5 to +10 s. Figure 1 illustrates the relative effect of changing the alert timing or the recovery strategy. The three strategies are shown with a 10-s forward-look alert and a 5-s delay in situ alert.

Table 1 shows that in one case (300-ft initial altitude, manual strategy, alert time zero) improving the alert time reduced the recovery altitude. In this instance, the delayed alert caused the recovery to begin in the boundary layer, below the altitude of maximum outflow. The early alert placed the airplane in a higher *F*-factor region for a significant portion of the recovery. This phenomena is not interpreted as suggesting that recoveries should intentionally be done below the maximum outflow altitude of microbursts or that alerts should be delayed for any reason. This phenomena and other results of the batch simulations are described in greater depth in Ref. 9.

Real-Time Simulation

The results seen in the batch simulations were substantiated in the piloted simulation runs. Given only the reactive alert, numerous crashes took place, whereas the lowest recovery altitude seen with the forward-look alert was 244 ft. The average recovery altitudes for the various combinations of the three factors are shown in Table 2. Examination of Table 2 shows that the difference in performance between the three recovery strategies was about 20 ft, whereas the difference in performance between the alert types was about 300 ft. Hence, the recovery altitude improvement produced by improving the alert time by 15 s was over an order of magnitude greater than what was achieved by changing the recovery strategy.

Figure 2 shows examples of aircraft trajectories during runs with the analytical model positioned 1600 ft from the runway. This geometry, the alert timing, and the recovery strategies are the same as the batch runs shown in Fig. 1. The characteristics of the recoveries agree well between the batch and real-time simulations. In both simulations, given a forward-look alert, the manual strategy initially produced a climb, followed by a descent at the stick shaker angle of attack. The other strategies produced a level trajectory that recovered at essentially the same altitude and with little or no time spent at the stick shaker angle of attack.

The pilots completed questionnaires and provided comments on the alerting and guidance. Of the seven pilots, six believed that the timeliness of the forward-alert was about right, whereas one believed that the alert was too late. When asked if the 10-s advance alert was sufficient to make a normal go-around procedure more appropriate than a programmed escape maneuver, six of the pilots said yes. The pilots were asked to rate the three recovery strategies in order of preference, with 1 assigned to the most preferred strategy. The averages for all the pilots were 1.3 for the flight-path angle strategy, 2.1 for the manual strategy, and 2.6 for the glide slope strategy.

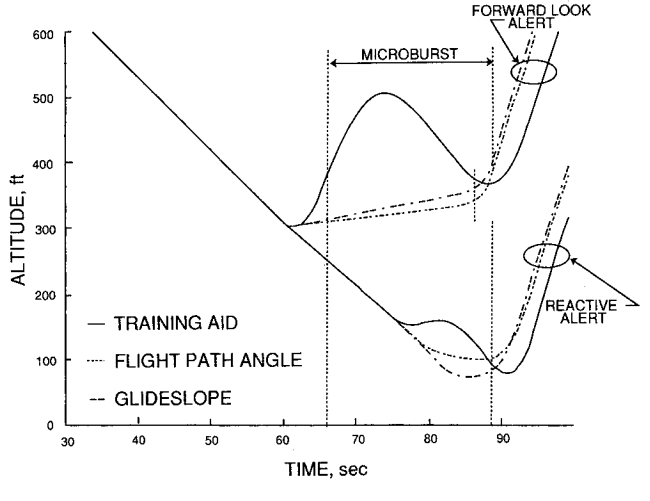

Fig. 1 Effect of forward-look capability and recovery strategy variation in batch simulation.

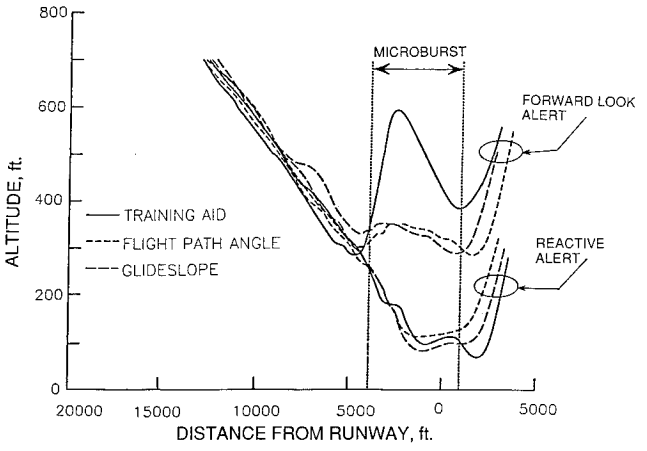

Fig. 2 Effect of forward-look capability and recovery strategy variation in piloted simulation.

Conclusions

Batch simulations and piloted simulations indicate that the factor that most strongly effects a microburst recovery is the time at which the recovery is initiated. In nearly all microburst situations evaluated in batch simulations, improving the alert time by 5 s provided a greater recovery performance increase than could be achieved by changing the recovery strategy. Forward-look alerts given 10 s prior to microburst entry permitted recoveries to made with negligible altitude loss. In piloted simulations, the average recovery altitude only varied about 20 ft between the recovery strategies tested. In contrast, the average recovery altitude varied nearly 300 ft between the two alert times tested (−5 and +10 s).

References

[1]Miele, A., Wang, T., Melvin, W. W., and Bowles, R. L., "Maximum Survival Capability of an Aircraft in a Severe Windshear," *Journal of Optimization Theory and Applications*, Vol. 53, No. 2, 1987, pp. 181–217.

[2]Hinton, D. A., "Flight-Management Strategies for Escape from Microburst Encounters," NASA TM-4057, August 1988.

[3]Hinton, D. A.,"Piloted-Simulation Evaluation of Recovery Guidance for Microburst Wind Shear Encounters," NASA TP-2886, DOT/FAA/DS-89/06, March 1989.

[4]Oseguera, R. M., and Bowles, R. L., "A Simple, Analytical 3-Dimensional Downburst Model Based on Boundary Layer Stagnation Flow," NASA TM-100632, July 1988.

[5]Boeing Company, "Wind Shear Training Aid, Volume 1—Overview Pilot Guide, Training Program," Boeing Commercial Airplane Co., Seattle, Washington, Contract DFTAO-1-86-C-00005, Feb. 1987.

[6]Miele, A., Wang, T., Tzeng, C. Y., and Melvin, W. W., "Optimization and Guidance of Abort Landing Trajectories in a Windshear," AIAA Paper 87-2341, Aug. 1987.

[7]Proctor, F. H., "The Terminal Area Simulation System, Volume I: Theoretical Formulation," NASA CR-4046, April 1987.

[8]Proctor, F. H., "The Terminal Area Simulation System, Volume II: Verification Cases," NASA CR-4047, April 1987.

[9]Hinton, D. A., "Relative Merits of Reactive and Forward-Look Detection for Wind-Shear Encounters During Landing Approach for Various Microburst Escape Strategies," NASA TM-4158, DOT/FAA/DS-89/35, Feb. 1990.